Appendix

The ion-coupling mechanism of human excitatory amino acid transporters

Juan C. Canul-Tec[1,2,3], Anand Kumar[1,2,3], Jonathan Dhenin[4], Reda Assal[1], Pierre Legrand[5], Martial Rey[4], Julia Chamot-Rooke[4] & Nicolas Reyes[1,2,3*]

[1]Membrane Protein Mechanisms Unit, Institut Pasteur, 25–28 rue du Docteur Roux, 75015 Paris, France

[2]Membrane Protein Mechanisms Group, European Institute of Chemistry and Biology, University of Bordeaux, 2 rue Robert Escarpit 33607 Pessac, France

[3]CNRS UMR 5234 Fundamental microbiology and pathogenicity, Bordeaux, France

[4]Mass Spectrometry for Biology Unit, CNRS USR 2000, Institut Pasteur, Paris 75015, France
[5]Synchrotron SOLEIL, L'Orme des Merisiers, 91192 Gif-sur-Yvette, France

[*]corresponding author

Content:

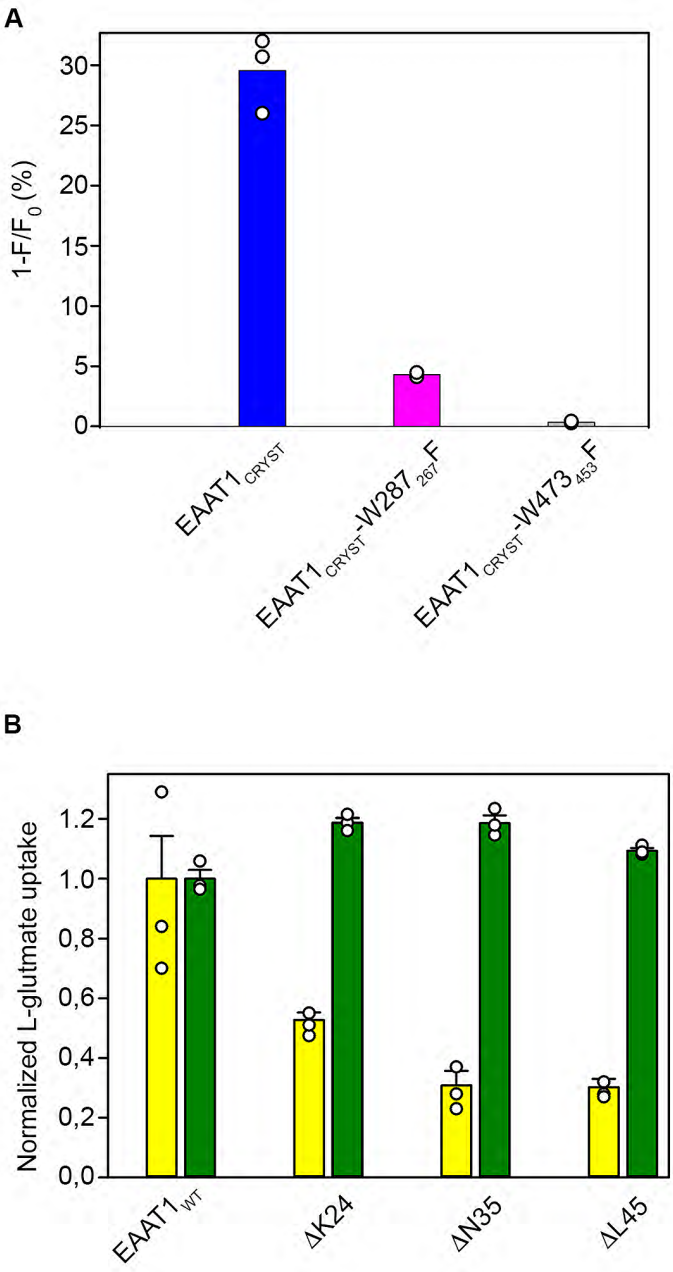

Appendix Figure S1 Effect Trp to Phe mutations on intrinsic-Trp fluorescence, and TM1a' deletions on transmitter transport.

A. Percentage of L-asp/Na^+ induced total fluorescence change ($1\text{-}F/F_0$). Individual phenylalanine mutations of $W287_{267}$ and $W473_{453}$ greatly decreased and abolished, respectively, Trp-intrinsic fluorescence associated to L-asp/Na^+ binding. Bar plots depict averages of at least two independent experiments (empty circles) performed in duplicates.

B. Radioactive L-glutamate uptake by HEK293 cells expressing $EAAT1_{WT}$-GFP fusion, and N-term truncations of this construct (labeled with the N-term residue). L-glutamate uptake decreases steeply in incremental N-term truncated constructs (radioactive counts, yellow bars), while protein expression (GFP counts, green bars) remain relatively constant compared to $EAAT_{WT}$. Bar plots depict averages and s.e.m. of three independent experiments (empty circles) performed in duplicates.

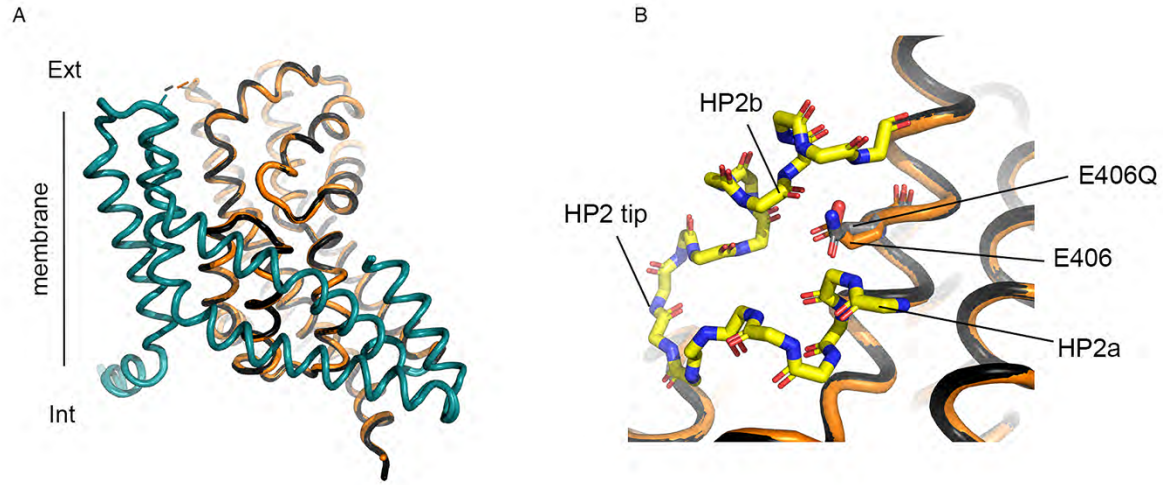

Appendix Figure S2 Transmitter-bound EAAT1$_{CRYST}$-E406$_{386}$Q structure
A. Superimposition of Na^+/transmitter-bound EAAT1$_{CRYST}$ (tranD orange) and EAAT1$_{CRYST}$-E406$_{386}$Q (tranD black) structures.
B. 406$_{386}$ sidechains adopt similar positions in the two structures, consistent with H-bonding between protonated E406$_{386}$ and residues in HP2b (yellow).

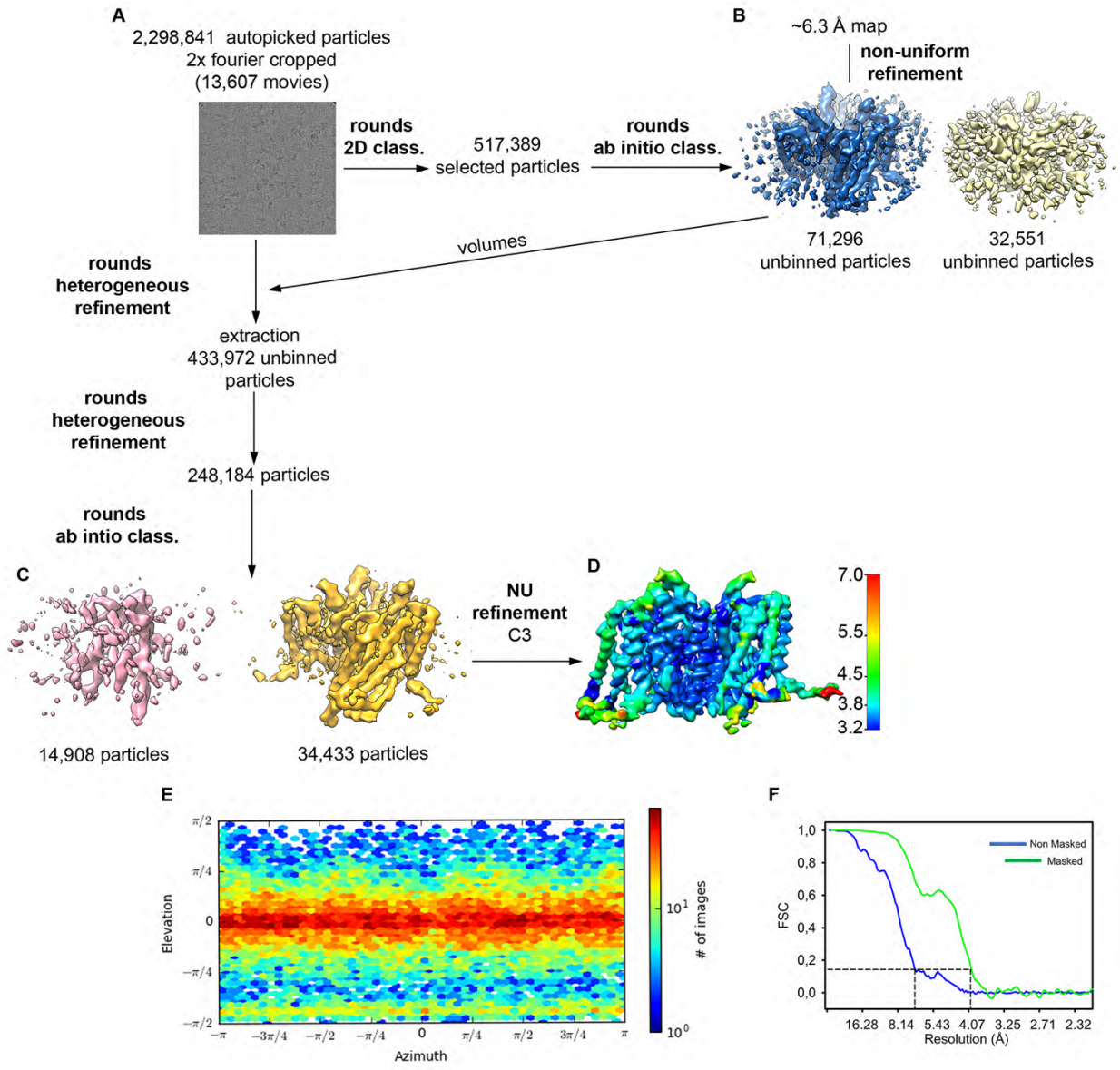

Appendix Figure S3 Overview cryo-EM data processing pipeline using cryoSPARC for EAAT1$_{WT}$ structure determination.

A. Representative EM micrograph.

B. First 3D *ab initio* classes used for heterogenous refinements.

C. Final 3D *ab initio* classes.

D. Refined and B-factor sharpened EM map colored by local resolution estimation.

E. Viewing direction distribution plot corresponding to C3-symmetric map shown in (D) after non-uniform refinement.

F. Fourier shell correlation (FSC) plot calculated in cryoSPARC with intercepts (dashed lines) at FSC 0.143.

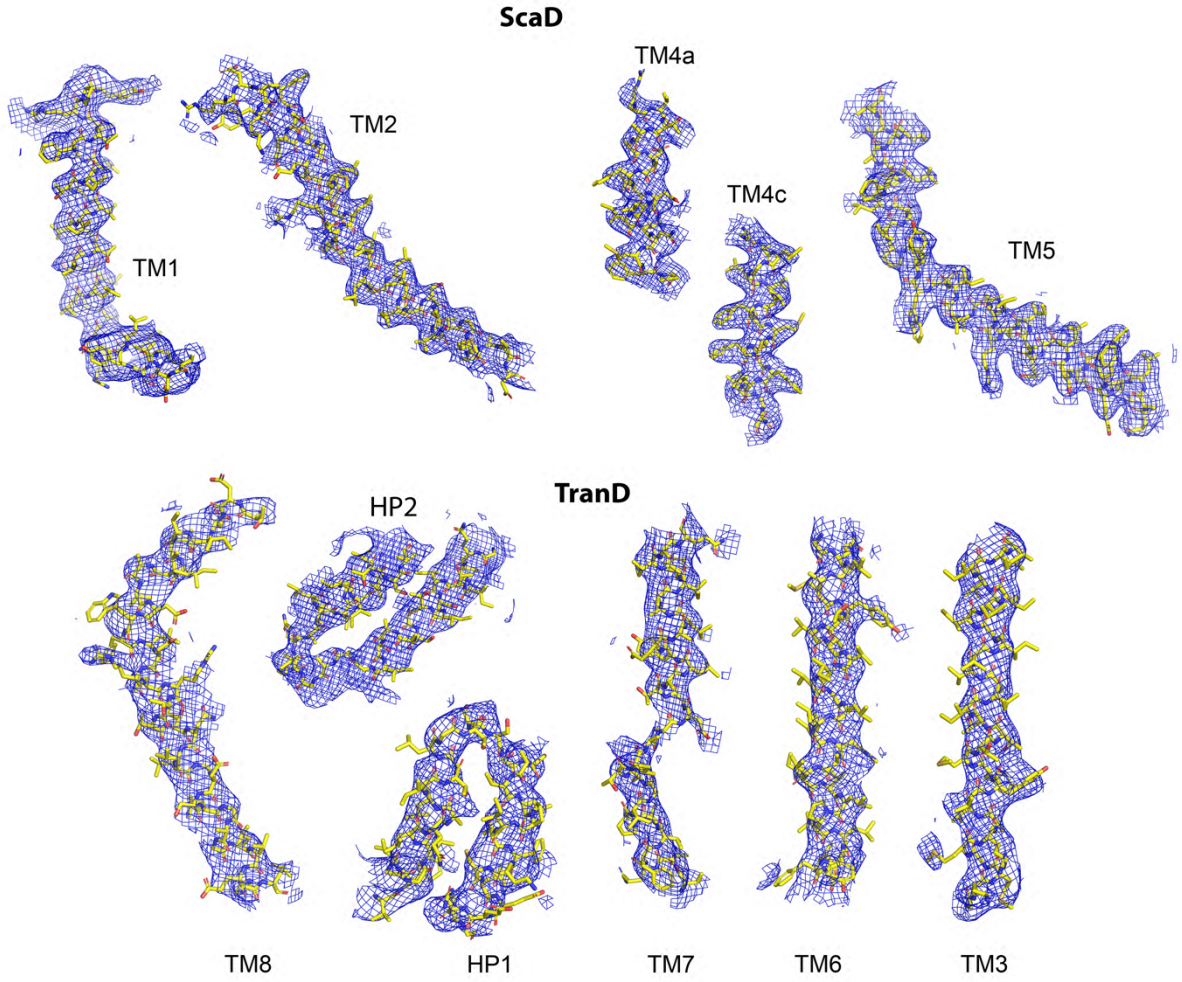

Appendix Figure S4 CryoEM density in EAAT1$_{WT}$ structure
CryoEM density around transmembrane helices in scaD and tranD, respectively.

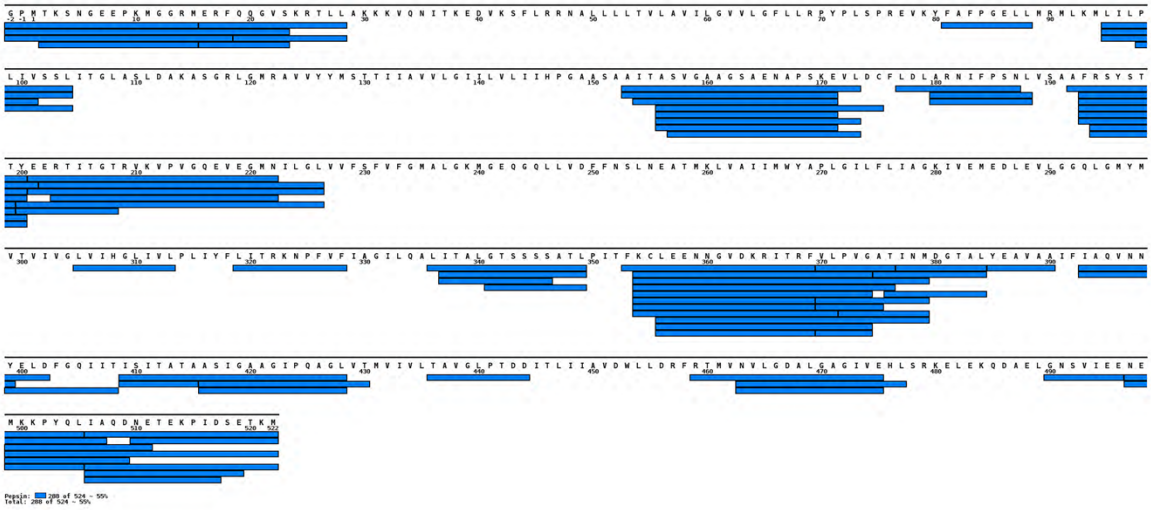

Appendix Figure S5 EAAT1$_{CRYST}$ HDX-peptide coverage map
77 peptides covering 55% of the EAAT1$_{CRYST}$ sequence were selected for HDX-MS analysis. Each bar below the protein sequence corresponds to a unique peptide. Amino acid numbering of the transporter starts at methionine. Two N-terminal residues (GP) remain after protease treatment during protein purification, and residue numbers correspond to EAAT1$_{CRYST}$ sequence. The map was generated with MSTools (https://www.hxms.com/mstools).

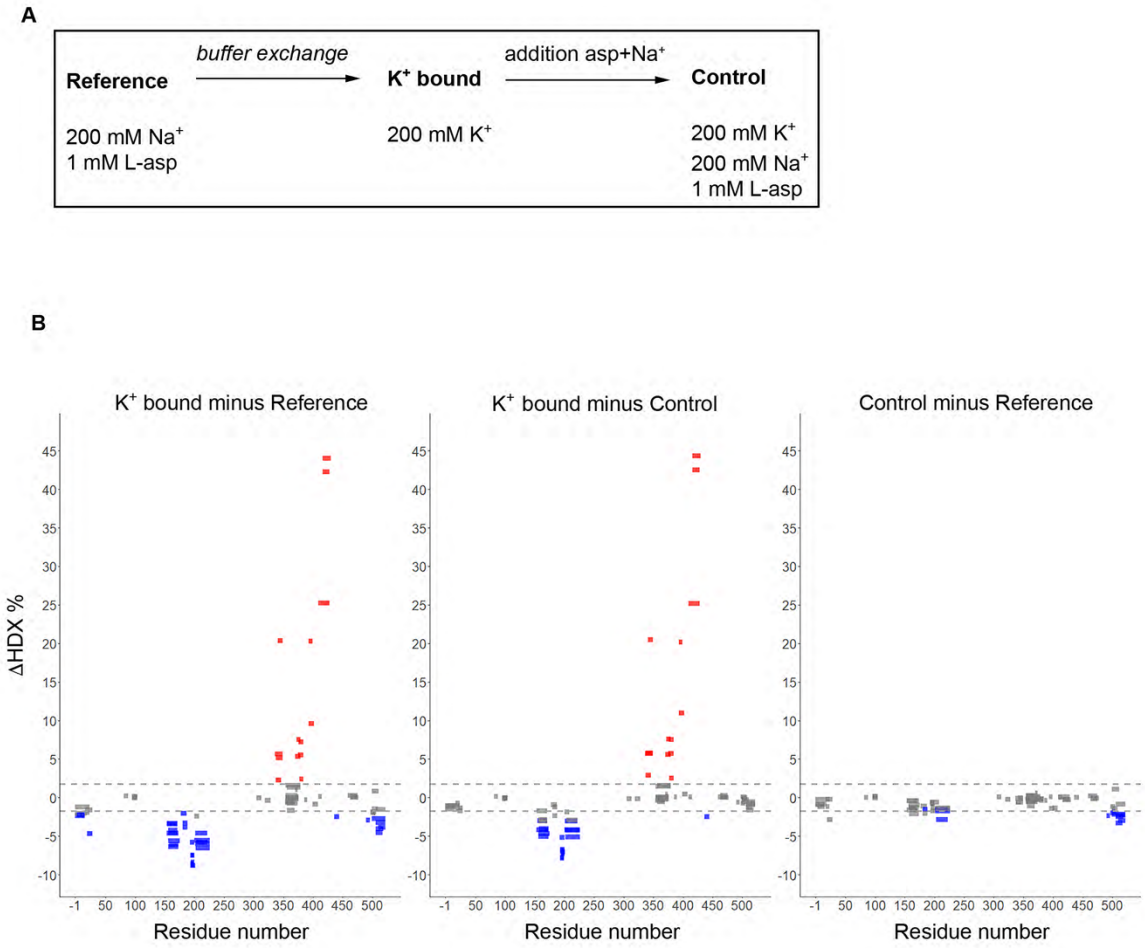

Appendix Figure S6 Reversible K^+-induced HDX changes

A. Schematic of HDX experimental setup indicating cation and ligand concentrations (see also methods).

B. Woods plots depicting percentage deuteration changes (ΔHDX %) of monitored peptides across $EAAT1_{CRYST}$ sequence. ΔHDX % values were generated by subtraction of deuterium uptake values between pairs of transporter states as indicated in each plot. Peptides exhibiting significant increase and decrease deuterium uptake are coloured red and blue, respectively, and those showing no significant changes in grey.

	$EAAT1_{CRYST}$ Na^+/L-asp and $UCPH_{101}$ bound	$EAAT1_{CRYST}$-E386Q Na^+/L-asp and $UCPH_{101}$ bound	$EAAT1_{CRYST}$ Rb^+/Ba^{+2} and $UCPH_{101}$ bound
Data collection			
Space group	$P6_3$	$P6_3$	$P6_3$
Cell dimensions			
a=*b*, *c* (Å)	122.88, 90.03	123.99, 90.80	124.24, 91.22
α=β, γ (°)	90.0, 120.0	90.0, 120.0	90.0, 120.0
Wavelength (Å)	0.979	0.979	0.815
Resolution (Å)	45.81-**3.25** (3.33-3.25)	46.21-**3.60** (3.69-3.60)	46.34-**3.92** (4.03-3.92)
Measured reflections	166319 (11129)	199896 (9786)	148439 (10475)
Unique reflections	12293 (887)	9313 (681)	7264 (519)
Completeness (%)	99.8 (98.1)	99.9 (99.9)	99.8 (98.5)
Completeness^{STARANISO} (%)	79.3 (28.6)	83.2 (37.2)	81.5 (39.5)
$I/\sigma(I)$	8.8 (0.4)	8.3 (0.5)	11.3 (0.6)
$I/\sigma(I)^{STARANISO}$	12.1 (1.3)	11.1 (1.2)	13.8 (1.4)
$CC_{1/2}$	0.99 (0.17)	0.99 (0.3)	1.00 (0.55)
$CC_{1/2}^{STARANISO}$	0.99 (0.52)	0.99 (0.62)	0.99 (0.62)
Redundancy	13.5 (12.5)	21.5 (14.4)	20.4 (20.1)
Redundancy^{STARANISO}	13.7 (14.3)	21.9 (14.5)	20.5 (20.0)
$R_{merge}^{STARANISO}$	0.13 (2.3)	0.14 (2.0)	0.10 (2.4)
Anisotropy direction$^{\$}$			
Resolution			
Overall (Å)	3.25	3.60	3.92
along h, k axis (Å)	3.67	3.60	4.01
along l axis (Å)	**3.25**	**3.60**	**3.92**
Refinement			
Resolution cut-off (Å)	23.31-**3.25**	28.0-**3.60**	21.85-**3.92**
No. of work/test reflections	9675/440	7703/394	5860/294
R_{cryst}/R_{free} (%)	21.9/23.8	22.4/26.8	23.0/27.8
No. of protein atoms	3135	3100	2973
No. of heteroatoms	45	44	35
Average *B* factors (Å^2)			
Protein	135.7	109.0	148.3
Heteroatoms	114.2	85.5	142.1
R.m.s. deviations			
Bond lengths (Å)	0.01	0.009	0.009
Bond angles (°)	1.17	1.05	1.03

Appendix Table S1 X-ray data collection and refinement statistics. 5% of reflections were used for calculation of R_{free}.Values in parentheses are for the highest-resolution shell. Data collection statistics were extracted with AIMLESS before and after anisotropic correction with STARANISO.

	$EAAT1_{CRYST-II}$ Rb^{+}/Ba^{+2} and $UCPH_{101}$ bound	$EAAT1_{CRYST-II}$ Ba^{+2} and $UCPH_{101}$ bound
Data collection*		
Space group	$P6_3$	$P6_3$
Cell dimensions		
a=*b*, *c* (Å)	124.38, 91.44	124.94, 92.02
$\alpha=\beta, \gamma$ (°)	90.0, 120.0	90.0, 120.0
Wavelength (Å)	0.979	0.979
Resolution (Å)	46.41-**3.91** (4.01-3.91)	46.64-**3.70** (3.80-3.70)
Measured reflections	123824 (8035)	181351 (13388)
Unique reflections	7403 (549)	8827 (657)
Completeness (%)	99.8 (99.1)	99.9 (99.8)
$Completeness^{STARANISO}$ (%)	63.4 (25.4)	74.7 (30.3)
$I/\sigma(I)$	9.0 (0.3)	11.3 (0.5)
$I/\sigma(I)^{STARANISO}$	15.7 (1.6)	15.5 (1.9)
$CC_{1/2}$	1.00 (0.15)	0.99 (0.43)
$CC_{1/2}^{STARANISO}$	1.00 (0.37)	0.99 (0.72)
Redundancy	16.7 (14.6)	20.5 (20.3)
$Redundancy^{STARANISO}$	17.0 (16.2)	20.6 (20.1)
$R_{merge}^{STARANISO}$	0.09 (2.2)	0.10 (2.3)
Anisotropy direction[$]		
Resolution		
Overall (Å)	3.91	3.70
along h, k axis (Å)	4.87	4.06
along l axis (Å)	**3.91**	**3.70**
Refinement		
Resolution cut-off (Å)	23.0-**3.91**	22.00-**3.70**
No. of work/test reflections	4632/228	6520/319
R_{cryst}/R_{free} (%)	24.6/29.1	23.7/28.5
No. of protein atoms	2933	2953
No. of heteroatoms	35	34
Average *B* factors (Å^2)		
Protein	149.4	164.9
Heteroatoms	152.9	158.3
R.m.s. deviations		
Bond lengths (Å)	0.009	0.009
Bond angles (°)	1.00	1.04

Appendix Table S2 X-ray data collection and refinement statistics. 5% of reflections were used for calculation of R_{free}.Values in parentheses are for the highest-resolution shell. Data collection statistics were extracted with AIMLESS before and after anisotropic correction with STARANISO.

	$EAAT1_{WT}$
Data collection	
Sample	EAAT1
Microscope	FEI Titan Krios
Voltage (kV)	300
Detector	Gatan K2-Summit
Energy Filter	EFTEM 165K
Electron dose ($e^-/Å^2$)	42.3
Defocus range (μm)	-2.0 to -0.8
Micrographs collected	13607
Software	CryoSPARC v3.1.0
Final Particle set (No.)	34,433
Resolution (Å)	3.99
FSC threshold	0.143
Sharpening B-factor	-126
Coordinate refinement and validation	
Initial model used (PDB ID)	7AWP, 6GCT
Software	PHENIX real_space_refinement
Model resolution (Å)	4.07
FSC threshold	0.143
Protein residues	1278
Non hydrogen atoms	9714
RMSD bonds (Å)	0.003
RMSD angles (°)	0.765
Ramachandran favored	96.65
Ramachandran allowed	3.35
Ramachandran outlier	0.0
Rotamer outlier	0.0
All atom clashscore	13.73
Mol Probity score	1.86

Appendix Table S3 Cryo-EM data collection and refinement statistics